Effect of Reynolds Number on the Aerodynamic Characteristics of Leading-Edge Protuberanced Airship Fin

S. Arunvinthan, C. Hari Babu, V. Manoj, and S. Nadaraja Pillai

1 Introduction

Lighter than aircraft (LTA) popularly known as airship is one of the first aircraft that realized humans dream of flight. Jean-Baptiste Meusnier proposed the first technical design of an airship featuring ellipsoidal shape with control surfaces like elevator and rudder in 1784 but lightweight powerful engine hindered his flight. Later with the advent of steam engine technology, during the year 1852, Henri Giffard incorporated steam engine technology in to airships for the first time and flew around 17 miles [1]. Even though these are some of the pioneering milestones in the history of airships, the golden age of airships began in 1900 with the launch of LZ1 Luftschiff Zeppelin of the German army. Subsequently, British and US forces began imitating its design and launch look alike airships named R-33, R-34 and Shenandoah (ZR-1) in the first half of 1900s. But with the advancements in the field of fixed wing aircraft progressing along with the occurrence of airship accidents including 1937 Hindenburg aircraft fire led to the downfall of the airships. Although the use of airships has been in recession for the past several years with the possibility of applying airships for military high-altitude long endurance surveillance and stationary airships design proposal as standby satellites has spurred interest among the researchers and this indicates the resurgence of the airship. Studies suggest that airships have wide variety of applications in telecommunication sector [2], surveillance (Stratospheric observation [3]; environmental monitoring [4]), terrain mapping [5] etc. Researchers realized

S. Arunvinthan (✉) · S. N. Pillai
Turbulence and Flow Control Lab, School of Mechanical Engineering, SASTRA Deemed to Be University, Thanjavur, Tamil Nadu 613401, India
e-mail: arunvinthan@mech.sastra.edu

C. H. Babu · V. Manoj
Department of Aeronautical Engineering—SMACE, Kalasalingam Academy of Research and Education, Krishnankoil, Tamil Nadu 626126, India

D. Shukla (ed.), *Lighter Than Air Systems*, Lecture Notes in Mechanical Engineering,
https://doi.org/10.1007/978-981-19-6049-9_14

that the flight behaviour of the airship depends upon the interaction between aerostatics and aerodynamics. Aerodynamics of the airship is one of the fundamental issues which have been investigated for many years but it has not been perfected yet. Airship designers have utilized wind-tunnel data to understand airship dynamics to a greater extent as it facilitates better design for airships. Such wind-tunnel test over the airships performed by Freeman [6] revealed that the tail fins not only produce lift force but also helps stabilizes the airship. Freeman identified that the hull of an airship experiences a nose-up pitch moment at nonzero angles of attack because of the normal force distribution at the front and the rear. Further, Freeman [7] reported that the fins attached to the hull of the airship produces 30–40% of the overall lift of an airship. Based on the wind-tunnel test performed by Curtiss [8], next to hull the second primary source of drag is due to the fins and the fins contribute around 7–27% of the total drag of the airship. Li et al. [9] confirmed this statement. Even though several studies were conducted on the drag reduction of the hull of an airship, to the extent of authors knowledge very few studies have been reported on the drag reduction of the fins of an airship. As we know that, nature offers the best solution to real-life problems as it has been optimized by evolution, it's time to look back to nature for answers. It is not new that aerodynamic designers draw inspiration from nature. In this present study, the nature-based inspiration has been drawn from humpback whale flippers. Frank E. Fish [10, 11] initiated the research on the flippers of the humpback whales and found out that the unique leading-edge protuberances present over its flippers offer aerodynamic benefits. To identify the uniqueness of such flippers with leading-edge protuberances, Fish conducted study over idealized flipper models with and without LEP and reported that flipper models with LEP experiences 25% more airflow than the flipper model without LEP. Subsequently, Fish [12–15] published several papers to his credit and also patented this technology. Further, wind-tunnel studies carried out by Miklosovic et al. [16] confirmed this behaviour. Following which, several researchers like Johari et al. [17], Custodio et al. [18] and Zhang et al. [19] conducted studies on leading-edge protuberances over NACA 63(4)-021 which closely resembles the aerofoil flippers and reported that the leading-edge protuberanced model outperforms the conventional straight blade model and is effective in drag reduction. Even though several studies have been performed over the LEP models, it should, however, be noted that no explicit study has been performed to investigate the effect of Reynolds number on the aerodynamic characteristics of such model to the extent of authors knowledge. Additionally, this will be the first of its kind in utilizing such LEP fins for airships to augment its aerodynamic efficiency by drag reduction. Recent study by Arunvinthan et al. [20] also confirmed that the modified LEP model also performs efficiently at various turbulence intensities. It is speculated that utilizing such modified LEP fins not only provide better aerodynamic performance characteristics but also aid in stabilized airship at various turbulence intensities.

2 Computational Methodology

NACA 63(4)-021 aerofoil profile has been chosen as the test model to evaluate the aerodynamic performance characteristics of leading-edge protuberanced (LEP)-based fin section for LTA. The NACA 63(4)-021 aerofoil has been chosen based on the framework of the previous researchers since it closely resembles the flippers of the humpback whale which acted as a source of bio-inspiration for the same. The leading-edge protuberances were modelled based on the sinusoidal pattern as outlined by Arunvinthan et al. [20] in his previous study. A schematic representation of the LEP test model is shown in Fig. 1. In this study, the primary focus is to identify the influence of the effect of Reynolds number on the aerodynamic characteristics on the leading-edge protuberanced fin section alone and hence, the variation of amplitude and wavelength of the leading-edge protuberances is kept constant throughout the study. Modified test model with leading-edge protuberances featuring amplitude of 0.12 °C and wavelength of 0.75°C is considered in this present study. To identify the Reynolds number effects, the test models were tested at various angles of attack ranging from 0^{o} to 45° in increment of 5° at various Reynolds number ranging between 10^2 and 10^6.

All the test models considered in this study were modelled using GAMBIT and analysed using commercial flow solver-ANSYS FLUENT. Based on the framework of the previous researchers, it has been identified that the first and the second order upwind methods were employed to solve the governing equations using semi-implicit method for pressure linked equation (SIMPLE). Standard $K - \epsilon$ turbulence model has been used for the numerical investigation as its two-equation model exhibits excellent predictive capability for problems dealing with aerofoil surfaces with least computational effort and challenges. In this study, the flow convergence criteria have

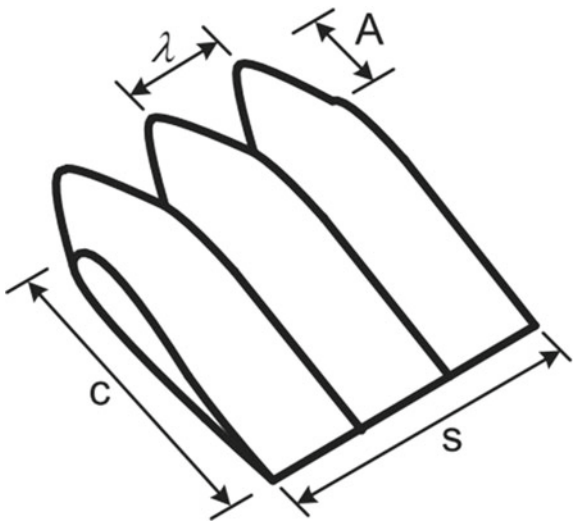

Fig. 1 Schematic representation of the modified LEP test model

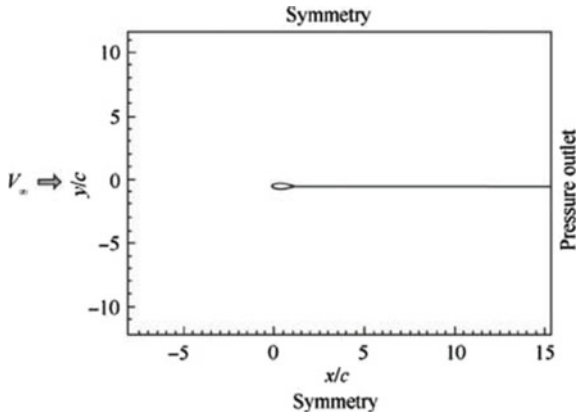

Fig. 2 Schematic representation of computational domain and boundary conditions

been set as 1×10^{-10} for all the computed quantities. The coordinate system is shown in the figure with the origin at the leading-edge point of the test model and correspondingly X, Y and Z axis measure the streamwise, lateral and spanwise directions, respectively. The fin model considered in this study possess a mean chord length 1 m. The length of the computational domain along the chordwise distance (L_C), normal to the chord (L_N) and the length of the computational domain in the lateral direction (L_Z) is of size 22.5C×20C×10C. The computational domain is designed large enough to rule out any unnecessary disturbances created by the boundaries. As this study involves complicated flow patterns over the modified LEP test model, it necessitated high-quality grids near the body surface and hence to generate an accurate mesh, algebraic initial point distribution has been used for surface grids. Likewise, grid independence test has been carried out for multiple sets of grids (0–1 million elements) with increasing mesh density of 0.2 million. Finally, 0.8 million elements were chosen as increasing the mesh density beyond this point exhibits independence in the results. In this study, the uniform inlet velocity boundary condition has been assumed on the inlet and the outlet is defined as the pressure outlet. No-slip boundary condition is set for the test model with LEP. Symmetry condition is set for lateral directions, respectively. A schematic representation of computational domain and boundary conditions is shown in Fig. 2.

3 Results and Discussion

3.1 Effect of Re on the Lift Characteristics Curve of LEP Fin

Figure 3 shows the variation of coefficient of lift (C_L) versus angle of attack (α) for the leading-edge protuberanced (LEP) test model at different Reynolds number. The results provide a quantitative measure of the aerodynamic performance of the LEP

models subjected to Reynolds number ranging between 10^2 and 10^6 at various angles of attack ranging from 0° to 45°. The effect of Re is evident from the lift coefficient plots that the characteristics regimes of flow over the leading-edge protuberanced test model shifts appreciably at different Reynolds number. It is evident from the figure that $\mathrm{Re} = 10^3$ exhibits the maximum lift coefficient in comparison against the other test Reynolds number. From the lift coefficient curve, it could be reported that the modified LEP test model exhibits better performance at low Reynolds number. At $\mathrm{Re} = 10^3$, it could be seen that the coefficient of lift (C_L) increases linearly with the increase in the angle of attack till $\alpha = 20°$ with a lift curve slope of 0.10 deg^{-1}, which then reduces to 0.6 deg^{-1} between 25° and 30°. Beyond which the increase in the coefficient of lift (C_L) is slowed down to 0.03 deg^{-1} between $30° \leq \alpha \leq 35°$, following which the stall phenomenon occurs with a slight dip in the lift curve. The difference in the lift curve slope experienced by the same LEP model subjected to different Reynolds number clearly indicates a change in the qualitative flow structure caused by the variation in Re. For instance, it can be seen from Fig. 3 that the same LEP model when subjected to $\mathrm{Re} = 10^6$ exhibits a lift curve slope of 0.10 deg^{-1} between $10° \leq \alpha \leq 15°$, following which the lift curve slope reduces to 0.02 deg^{-1} between $20° \leq \alpha \leq 25°$. It is of interest to note that the qualitative flow structure occurring over the same LEP model subjected to different Re tends to reduce the maximum lift coefficient. For instance, the maximum lift coefficient observed for the LEP test model when subjected to $\mathrm{Re} = 10^3$ is 3.44 at $\alpha = 40°$, whereas at $\mathrm{Re} = 10^6$ the maximum coefficient of lift reduces to 2.11 at $\alpha = 30°$. Henceforth, it is worth noting that with the increase in the Reynolds number, not only the decrease in the maximum lift coefficient is observed, but the angle of attack at which the maximum lift coefficient is attained is also significantly reduced. Even though, based on the lift coefficient plot, it can be claimed that the modified LEP test model is good at low Reynolds number compared to high Reynolds number, it should, however, be noted that at high Re, the modified LEP model offers sustained lift coefficient over large range of angle of attack. For instance, at $\mathrm{Re} = 10^6$ the test model offers sustained lift coefficient between $20° \leq \alpha \leq 45°$ which is way higher than the conventional straight fin model for the lighter than air aircraft. To better understand the aerodynamic characteristics of this modified LEP test model, it becomes quintessential to understand the drag and the aerodynamic efficiency as well.

3.2 Effect of Re on the Drag Characteristics Curve of LEP Fin

Figure 4 represents the variation of coefficient of drag at every test angle of attack. Contrary to the lift coefficient plots the modified LEP test model subjected to high Reynolds number exhibits the lowest drag coefficient in comparison against the low Reynolds number. Therefore, it can be reported that the increase in the Reynolds number tends to decrease the drag coefficient between 10^2 and 10^6 at various angles

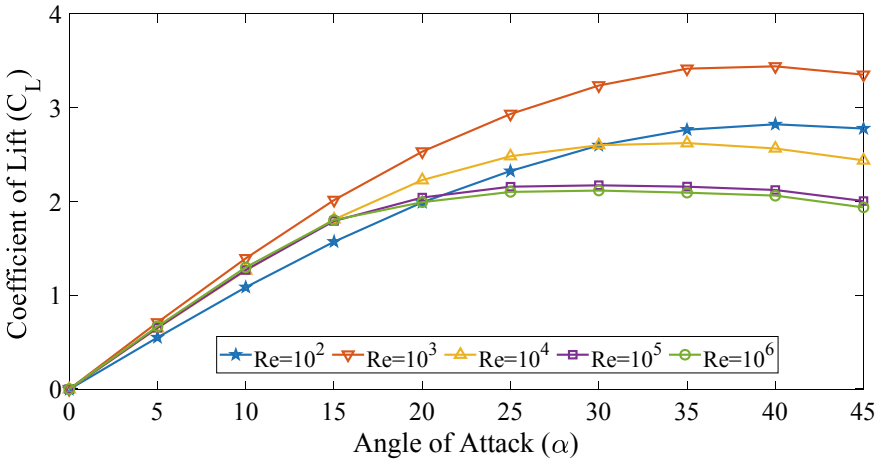

Fig. 3 Coefficient of lift (C_L) versus angle of attack (α) for LEP fin

of attack. It is believed that the increase in the momentum provided by the increase in the flow velocity accompanied with the increase in the Reynolds number might be the plausible reason behind the decrease in the drag coefficient with the increase in the Re. One might speculate that the decrease in the drag coefficient can be caused by the delayed flow separation caused by the increase in Reynolds number.

To get further insight in to this, the surface pressure distribution over the modified leading-edge protuberanced models needs to be investigated. Since the modified leading-edge protuberanced model is not a constant chord model, the surface pressure distribution needs to be investigated at various chordwise locations namely the peak

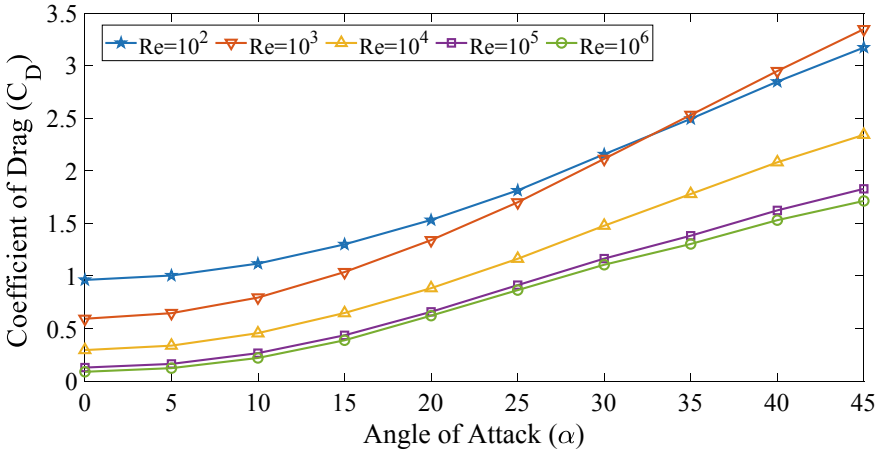

Fig. 4 Coefficient of drag (C_D) versus angle of attack (α) for LEP fin

where the chord maxima occur, mid and trough where the chord minima occur. As stated above, the surface pressure distribution over the modified leading-edge protuberanced models was obtained at peak, mid and trough sections and are displayed in Fig. 5a–c, respectively, for $\alpha = 10°$. In order to understand the influence of the Reynolds number effect on the aerodynamic characteristics, the peak section of the test model subjected to different Reynolds number is plotted in same graph. Likewise, the mid and trough section of the test model subjected to different Re is also plotted in individual graphs for better understanding. In addition, this will help us understand the flow physics to a greater extent. It is evident from the surface pressure distribution of peak, mid and the trough section, that the trough exhibits the maximum negative suction pressure signifying that the maximum velocity is attained over the trough section compared to the peak and the mid. Since the primary aim of the study is to identify the effect of Re, the variation of surface pressure distribution with Re is then observed. Generally, the oncoming flow is bifurcated at the leading edge of an aerofoil and then one flow will move over the upper surface of an aerofoil and the other one will move over the lower surface of an aerofoil. The flow which is moving over an upper surface of the aerofoil gradually accelerates indicated by the negative suction pressure (i.e. the favourable pressure gradient) and then, the pressure keeps on increasing with the increase in the x/C till the trailing edge and achieves pressure recovery (i.e. tends to get equal to the ambient pressure zero). It is identified from the graphs that the Re influences the flow characteristics prevailing over the upper surface of the aerofoil. In other words, with the increase in Re, the chordwise distance taken to achieve the maximum negative suction pressure (favourable pressure gradient) reduces. For instance, it can be seen from the Fig. 5b that at surface distribution of mid sections, at $\mathrm{Re} = 10^2$ the maximum negative suction peak is reached at $x/C = 0.31$ whereas for $\mathrm{Re} = 10^3$ it happens at $x/C = 0.24$ and for $\mathrm{Re} = 10^4$ the peak suction pressure is at $x/C = 0.20$, respectively. It is of interest to note that at $\mathrm{Re} = 10^5$ and 10^6 there is no advancement in the chordwise distance rather the increase in the maximum negative suction pressure is observed. At both $\mathrm{Re} = 10^5$ and 10^6, the peak negative suction pressure is observed at $x/C = 0.13$. Similar trend line has been observed in the peak and the trough sections also. Therefore, it becomes clear that with the increase in the Re, the maximum negative suction pressure (favourable pressure gradient) tends to move towards the vicinity of the leading edge, thus providing reduced drag coefficient. As aerodynamic efficiency not only depends on drag reduction, the ratio of lift to drag (i.e. aerodynamic efficiency) needs to be understood for better insight.

The aerodynamic efficiency (L/D) vs. angle of attack is presented in Fig. 6. It is evident from the figure that $\mathrm{Re} = 10^6$ exhibits peak aerodynamic efficiency over the test angles of attack especially in the pre-stall region. Following which $\mathrm{Re} = 10^5$ exhibits the second peak and successively drops down to $\mathrm{Re} = 10^2$ finally. This clearly shows that the modified LEP test model exhibits good aerodynamic efficiency at $\mathrm{Re} = 10^5$ and 10^6 and hence could be used for LTA fin sections. The surface pressure distribution plots are further investigated in detail to observe more peculiar phenomenon like laminar separation bubble, etc., and the presence of the same if exists will be reported in the conference.

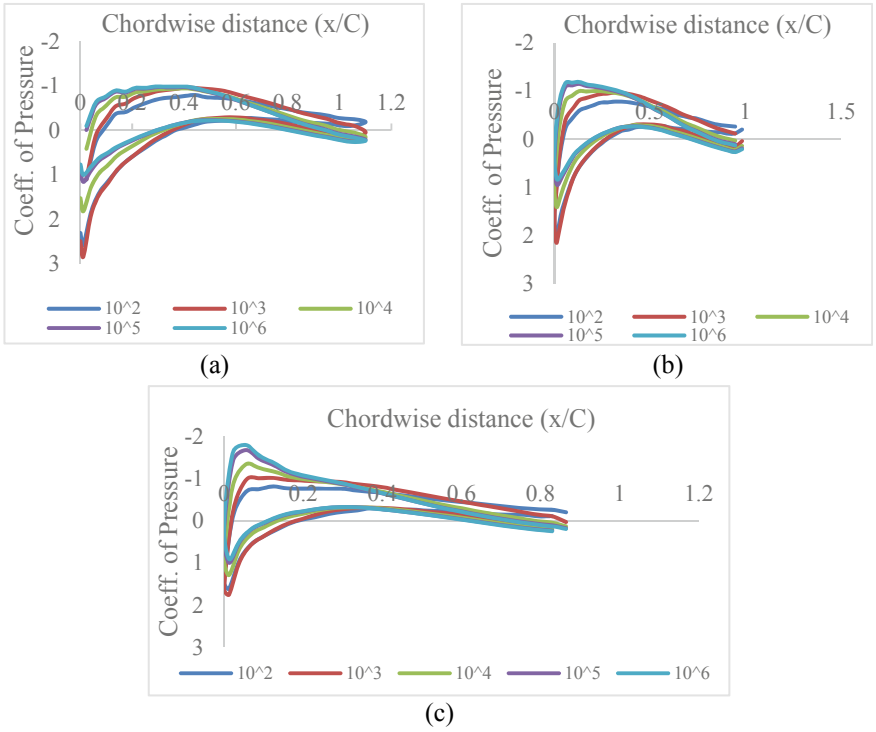

Fig. 5 Coefficient of pressure (C_p) versus chordwise distance (x/C) for **a** peak, **b** mid and **c** trough

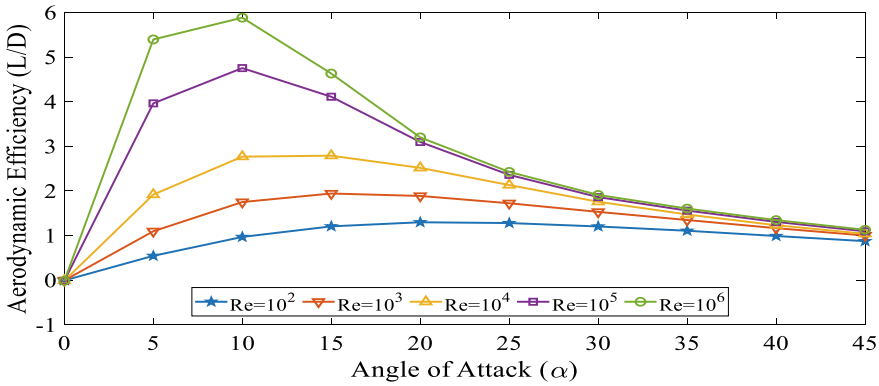

Fig. 6 Aerodynamic efficiency (L/D) versus angle of attack (α)

4 Conclusion

In this paper, the computational investigation of the effect of Reynolds number (Re) on the aerodynamic characteristics of the leading-edge protuberanced (LEP) fins at wide range of angles of attack ranging from 0 to 45° is computationally evaluated. The aerodynamic force coefficients, aerodynamic efficiency and surface pressure distribution were investigated in detail and based on the results the following conclusions were made:

1. Aerodynamic force coefficients like (C_L) and (C_D) of the leading-edge protuberanced fin section are significantly influenced by the Reynolds number.
2. Leading-edge protuberanced fin section subjected to Re = 10^6 shows the minimum drag coefficient and maximum aerodynamic efficiency when compared against the other test cases.
3. With the increase in the Reynolds number, the favourable pressure gradient (i.e. peak negative suction pressure) tends to move towards the vicinity of the leading edge, thus providing better aerodynamic characteristics and reduced drag.
4. Surface pressure distribution over the peak, mid and the trough section shows that the peak negative suction pressure exists at trough region, thus showing that majority of the flow goes through the trough region, thus inducing a spanwise pressure gradient among the upper surface of the aerofoil itself.

To gain better understanding, the study has to be made at multiple velocities in the same Reynolds number range itself. Attempts can be made in future to experimentally evaluate the aerodynamic characteristics of such LEP fins and flow visualization studies could also be performed to further ascertain this underlying flow physics.

References

1. Gerken LC (1990) Airships: history and technology. Chula Vista, CA: American Scientific Corporation; pp 1–19. Wilson JR (1990) A New era for airships. Aeros
2. Lee Y-G, Kim D-M, Yeom C-H (2006) Development of Korean high altitude platform systems. Int J Wireless Inf Netw 13(1):31–42
3. Lee S, Bang H (2007) Three-dimensional ascent trajectory optimization for stratospheric airship platforms in the jet stream. J Guid Control Dyn 30(5):1341–1352
4. Dorrington GE (2005) Development of an airship for tropical rain forest canopy exploration. Aeronaut J 109:361–372
5. Hygounenc E, Jung I, Soueres P, Lacroix S (2004) The autonomous blimp project of LAAS-CNRS: achievements in flight control and terrain mapping. Int J Robot Res 23(4–5):473–511
6. Freeman HB (1933) Force measurements on a 1/40-scale model of the U.S. Airship Akron. NACA TR-432
7. Freeman HB (1934) Pressure distribution measurements on the hull and fins of a 1/40-scale model of the U.S. Airship Akron. NACA TR-443
8. Curtiss HC, Hazen DC, Putman WF (2003) Experimental investigations on hull–fin interferences of the LOTTE airship. Aerosp Sci Technol 7(8):603–610
9. Li Y, Nahon M, Sharf I (2011) Airship dynamics modelling: a literature review. Prog Aerosp Sci 47:217–239

10. Fish FE (1994) Influence of hydrodynamic-design and propulsive mode on mam-malian swimming energetics. Aust J Zool 42:79–101
11. Fish FE, Battle JM (1995) Hydrodynamic design of the humpback whale flipper. J Morphol 225:51–60
12. Fish FE, Lauder G (2006) Passive and active flow control by swimming fishes and mammals. Annu Rev Fluid Mech 38:193–224
13. Fish FE, Howle LE, Murray MM (2008) Hydrodyn flow control mammals. Integr Comp Biol 48:788–800
14. Fish FE, Weber PW, Murray MM, Howle LE (2011) Marine applications of the biomimetic Humpback whale flipper. Mar Technol Soc J 45:198–207
15. Fish FE, Weber PW, Murray MM, Howle LE (2011) The tubercles on humpback whales flippers: application of bio-inspired technology. Integr Comp Biol 51:203–213
16. Miklosovic D, Murray M, Howle LE, Fish FE (2004) Leading-edge tubercles delay stall on humpback whale (megaptera novaeangliae) flippers. Phys Fluids 16:L39–L42
17. Johari H, Henoch CW, Custodio D, Levshin A (2007) Effects of LEP on airfoil perf. AIAA J 45:2634–2642
18. Custodio D, Henoch C, Johari H (2012) Aerodynamic characteristics of finite-span wings with leading-edge protuberances. In: Proceedings of 50th AIAA aerospace sciences meeting including the new horizons forum and aerospace exposition, Nashville, Tennessee. AIAA. 54, pp 1–12
19. Zhang M, Wang G, Xu J (2013) Aerodynamic control of low-Reynolds-number airfoil with leading-edge protuberances. AIAA J 51:1960–1971
20. Arunvinthan S, Nadaraja Pillai S, Cao S (2020) Aerodynamic characteristics of variously modified LEP wind turbine blades under various turbulence intensities. J Wind Eng Indust Aerodyn 202:104–188